

Transmission electron microscopy and atomic force microscopy characterization of nickel deposition on bacterial cells

WANG Jing, HE ShiYing, XU LiNa & GU Ning[†]

Jiangsu Laboratory for Biomaterials and Devices, National Laboratory of Molecular and Biomolecular Electronics, Department of Biological Science and Medical Engineering, Southeast University, Nanjing 210096, China

Recently bacterial cells have become attractive biological templates for the fabrication of metal nanostructures or nanomaterials due to their inherent small size, various standard geometrical shapes and abundant source. In this paper, nickel-coated bacterial cells (gram-negative bacteria of *Escherichia coli*) were fabricated via electroless chemical plating. Atomic force microscopy (AFM) and transmission electron microscopy (TEM) characterization results reveal evident morphological difference between bacterial cells before and after deposition with nickel. The bare cells with smooth surface presented transverse outspreading effect at mica surface. Great changes took place in surface roughness for those bacterial cells after metallization. A large number of nickel nanoparticles were observed to be equably distributed at bacterial surface after activation and subsequent metallization. Furthermore, ultra thin section analytic results validated the presence and uniformity of thin nickel coating at bacterial surface after metallization.

biotemplate, atomic force microscopy (AFM), transmission electron microscopy (TEM), metallization, bacterial cell

Over the past few years, metallic nanostructures or nanomaterials have attracted great attention of scholars and scientists all over the world owing to their potential applications in electronics, mechanics, optics and sensors^[1,2]. Recently synthesis and fabrication of metallic nanostructures or nanomaterials based on biological templates have become a novel and attractive trend. Among other biological templates such as DNA^[3-5], microtubules^[6,7], S-layer protein^[8], protein cages^[9] and natural pollen particles^[10], bacterial cells have become attractive candidates for their inherent small size (about 1 μm), various standard geometrical shapes (such as spherical, bacilliform, tubular, gyroidal, corn-shaped or banana-shaped) and abundant source. It is quite difficult to fabricate such small standard three-dimensional metallic nanostructures even with some available micro-machining methods. The bacteria templates chosen for the fabrication of metal nanomaterials are currently

mainly focused on some gram-positive bacteria^[11-13]. Herein *Escherichia coli*, a typical kind of gram-negative bacteria with straight rod shape, was used as the metallization template in our study.

From analytic results of modern techniques, it is a common knowledge that the surface properties of bacterial cell wall are mainly determined by proteins, polysaccharides, (lipo)teichoic acids and peptidoglycans^[14-16]. Compared with these analytic techniques, atomic force microscopy (AFM) has shown great advantages in surface science due to its high resolution, easy sample preparation and flexible working environments. Recently a lot of studies on the morphology and analysis on adhesion forces of bacteria and bacterial biofilms on

Received January 4, 2007; accepted April 22, 2007

doi: 10.1007/s11434-007-0390-y

[†]Corresponding author (email: guning@seu.edu.cn)

Supported by the National Natural Science Foundation of China (Grant Nos. 60171005, 60371027, 60121101, 20573019 and 90406023) and Open Project Foundation of Laboratory of Solid State Microstructures of Nanjing University

solid surfaces have been carried out using AFM^[17–19]. But to our knowledge, there have been few corresponding reports on the combination of AFM characterization with bacteria-templated metallic nanostructure.

In this paper, the method of electroless chemical plating was chosen to deposit nickel nanoparticles on bacterial surface. Due to no need of a current supply and no limitations on the types or shapes of substrates, it has been a promising method for fabricating uniform metal coating on any kind of substrate. The morphology of bare and metallized bacterial cells was observed and depicted using AFM. For contrast and validation, transmission electron microscopy and ultra thin section analysis were carried out at the same time. The objective of this study is to supply more detailed morphological information of bacteria-templated metal nanostructures for their potential applications in broad fields of nanoscience.

1 Materials and methods

1.1 Bacteria culture

Gram-negative bacteria of *Escherichia coli* (ATCC 25922) was chosen as biotemplates of metallization in our study. The pure culture of the bacteria was grown in Luria-Bertani (LB) medium for 5 h at 37°C. After cultivation, bacterial cells were collected by centrifugation and suspended in pure water.

1.2 Activation and nickel deposition on bacterial surface

Electroless deposition occurs in a redox process, where the cation of the metal deposited is chemically reduced. The redox process of electroless deposition takes place only on appropriate catalytic surfaces. Here tin-free chloride-rich Pd (II) solutions were chosen as activation initiator. It is hypothesized that the negatively charged lipopolysaccharide protruding out of cell wall supplies the possibility to bind with positively charged Pd ions via electrostatic interaction, which serves as further metallization nucleation sites. After treating with fresh Pd (II) solutions for 15 min at room temperature and washing with pure water at 10000 r/s centrifugation, electroless nickel deposition was carried out by mixing bacteria solution with appropriate volume of electroless nickel plating bath (pH = 11.7), containing NiSO₄·6H₂O 8 g/L, N₂H₄ 27 mL/L, C₄H₄O₆KNa 10 g/L, NaOH 5 g/L and some steady solvents, and reacting at 80°C. After 20 min, the ultimate product was obtained by centrifug-

ing and washing with water for several times.

1.3 AFM characterization

A Nanoscope IIIa AFM (Digital Instruments, Santa Barbara, CA, USA) operating in contact mode in air was used to image bacterial cells. The relative humidity was 50%–60% and no capillary forces were observed during AFM operation. The nanoprobe cantilevers made of silicon nitride (Si₃N₄) have a spring constant of $K = 0.06$ N/m (Digital Instruments). The Digital Nanoscope software (version 4.32) was used to analyse topographic images of cell surface. For simplify and comparability, all ultimate analytic AFM numeric values were corrected to 0.1 nm. All AFM images were only treated with flatten command. For sample preparation, freshly cleaved mica surface was chosen as the substrate. A ~40 μL sample solution was pipetted onto mica disk for 10 min, rinsed in pure water and allowed to dry for imaging and analyses. Except for special indication, all samples were freshly prepared from the same group and characterized within a drying period of 4 h for assuring the comparability among those samples after different treatments to the largest extent.

1.4 TEM and ultra thin section TEM characterization

For contrast and validation, a TEM (Hitachi JEOL, Japan) was used. For ultra thin section samples preparation, the collected metallized bacterial cells were firstly stored at room temperature for 3 h in glutaraldehyde liquor (3 % in concentration), and then rinsed thoroughly with phosphoric acid. After that, they were collected and stored at room temperature for 3 h with osmic acid (1 % in concentration). After dehydrating with acetone, soaking in epoxy propane, embedding and fixing with epoxy resin, ultra thin sections were prepared and characterized with TEM (H-600, Hitachi, Japan).

2 Results and discussion

2.1 TEM characterization of bare and metallized *E. coli* cells

Figure 1 shows TEM images of *E. coli* cells before and after metallization, respectively. As observed from Figure 1(a), several bare *E. coli* cells in the size of ~1 μm × 500 nm appear clear contour and smooth surface. Nickel deposition occurs quickly at the surface of bacterial cells after activation and subsequent treatment with nickel

plating bath within 30 s, whose diameter distributes mostly in the range of 4–6 nm (Figure 1(b) and (d)). With an increase in the metallization time period, both the distribution density and diameter of deposited nickel particles increase (Figure 1(c) and (e)). Some tiny local distribution ununiformity of nickel particles at bacterial

surface may be related to local activity difference, which leads to local deposition velocity difference of nickel particles, and gas flow during electroless plating^[10]. The ultra thin section TEM characterization further validates the existence and the uniformity of thin nickel coating at bacterial surface (Figure 2).

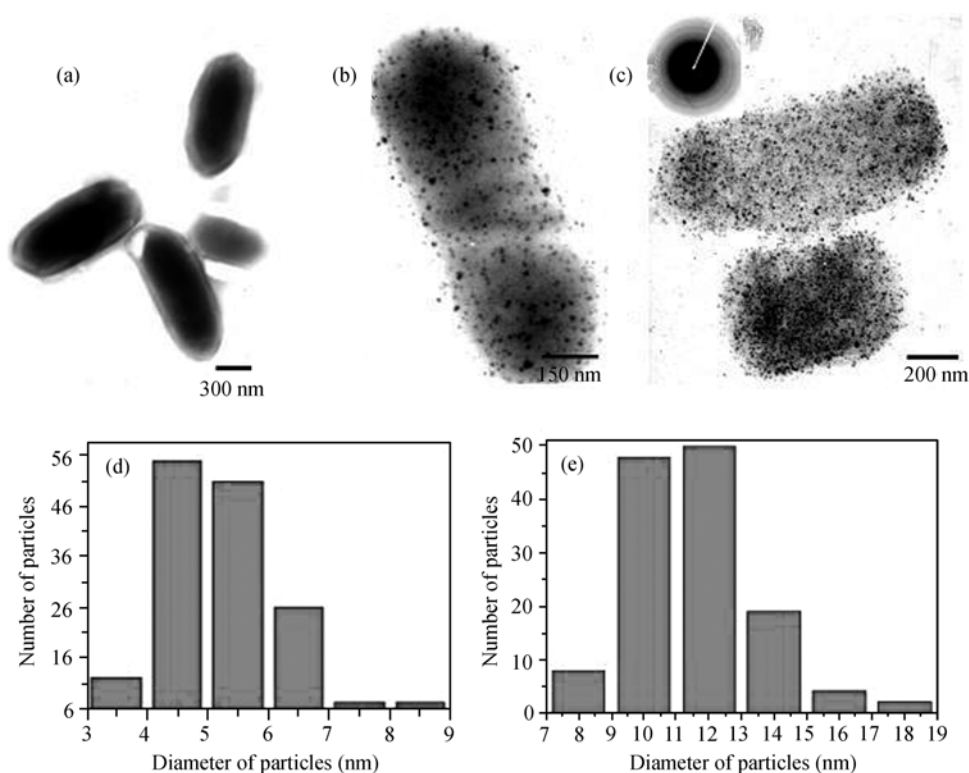


Figure 1 TEM images of bare and metallized bacterial cells. (a) Bare bacterial cells; (b) bacterial cells after Pd (II) activation and subsequent nickel deposition for 30 s; (c) bacterial cells after Pd (II) activation and subsequent nickel deposition for 15 min, the inset image is the electron beam diffraction, the scale bar = 300, 150, 200 nm, respectively; (d) and (e) are the histogram of size distribution of nickel particles from (b) and (c), respectively.

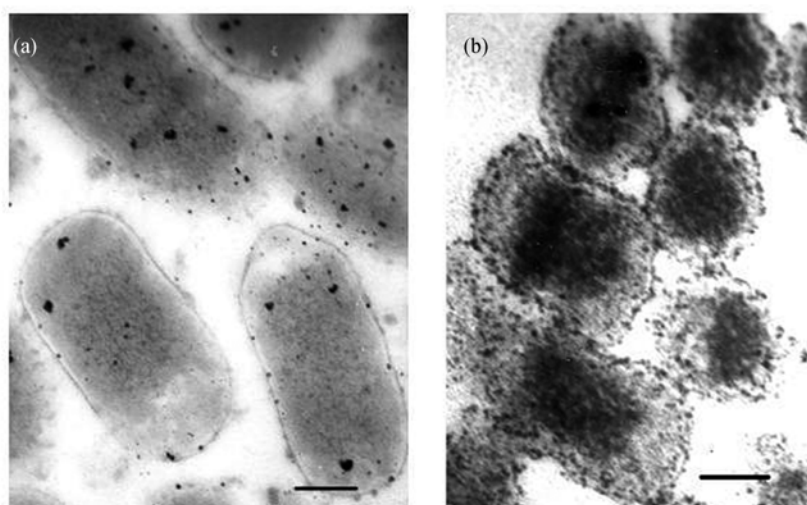


Figure 2 Ultra thin section TEM images of bare and metallized bacterial cells. (a) Bare bacterial cells; (b) bacterial cells after Pd (II) activation and subsequent nickel deposition for 15 min; in both images, the scale is 200 nm.

2.2 AFM characterization of bare and metallized *E. coli* cells

From Figure 3(a), one can see that AFM height image of dry *E. coli* cells adsorbed on mica surface, and a layer of biofilm made of *E. coli* cells can be observed. The cell surface is comparatively smooth, which has been approved by roughness analysis (Figure 3(c)). The arithmetic average roughness R_a and root mean square (RMS) roughness R_q within one *E. coli* cell surface are only 1.1 and 0.9 nm, respectively. The reason of choosing $\sim 300\text{ nm} \times 300\text{ nm}$ as the analytic area lies in the limitation of bacterial size and the need of making contrast between

bacterial cells under different conditions. Herein, the values of R_a and R_q for at least 50 random chosen bare and metallized bacterial cells were measured with surface analysis software, whose average values are listed in Figure 4. Some fine ripples can be seen at some bacterial cell surface due to their extrusion and dehydration (Figure 3(b)). The section analysis on arbitrarily chosen bare *E. coli* shows that its section curve is either rounded or semi-rounded, but arciform with an unproportionable ratio of height to width, being 60.3 to 781.3 nm. It is assumed to be related with the evident outspreading effect of bacterial cells due to their dehydration.

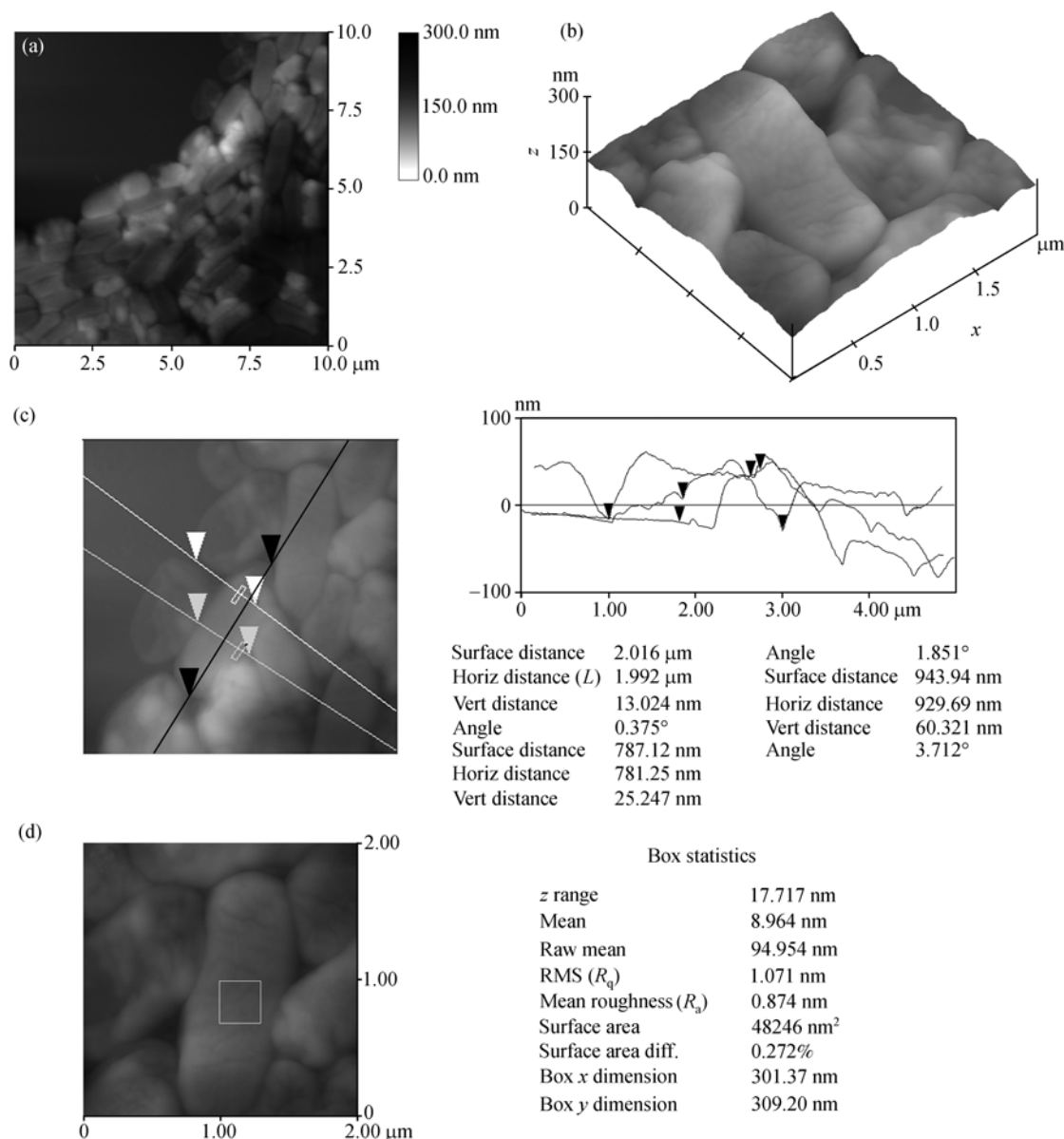


Figure 3 AFM characterization of bare *E. coli* cells. (a) Height image of a large area showing a biofilm of bare bacterial cells; (b) 3D height image of smaller area magnified from (a); (c) section analysis of one *E. coli* cell, whose 3D size is $1992.0 \times 781.3 \times 60.3\text{ nm}$; (d) surface roughness analysis of bare *E. coli* cells within $\sim 300\text{ nm} \times 300\text{ nm}$.

After metallization, plump bacterial cells are in good dispersal (Figure 5(a)). Compared with those bare bacterial cells, their surface becomes obviously coarse. A large number of nanoparticles can be clearly observed to

equally distribute at bacterial surface by AFM phase image (Figure 5(d)). The ratio of height to width of bacterial cells after metallization has increased, which shows 110.4 to 523.9 nm in Figure 5(c).

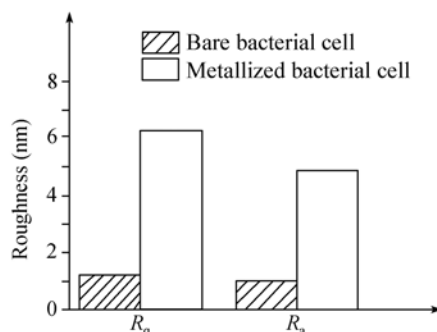


Figure 4 Surface roughness contrast between bare and metallized *E. coli* cells.

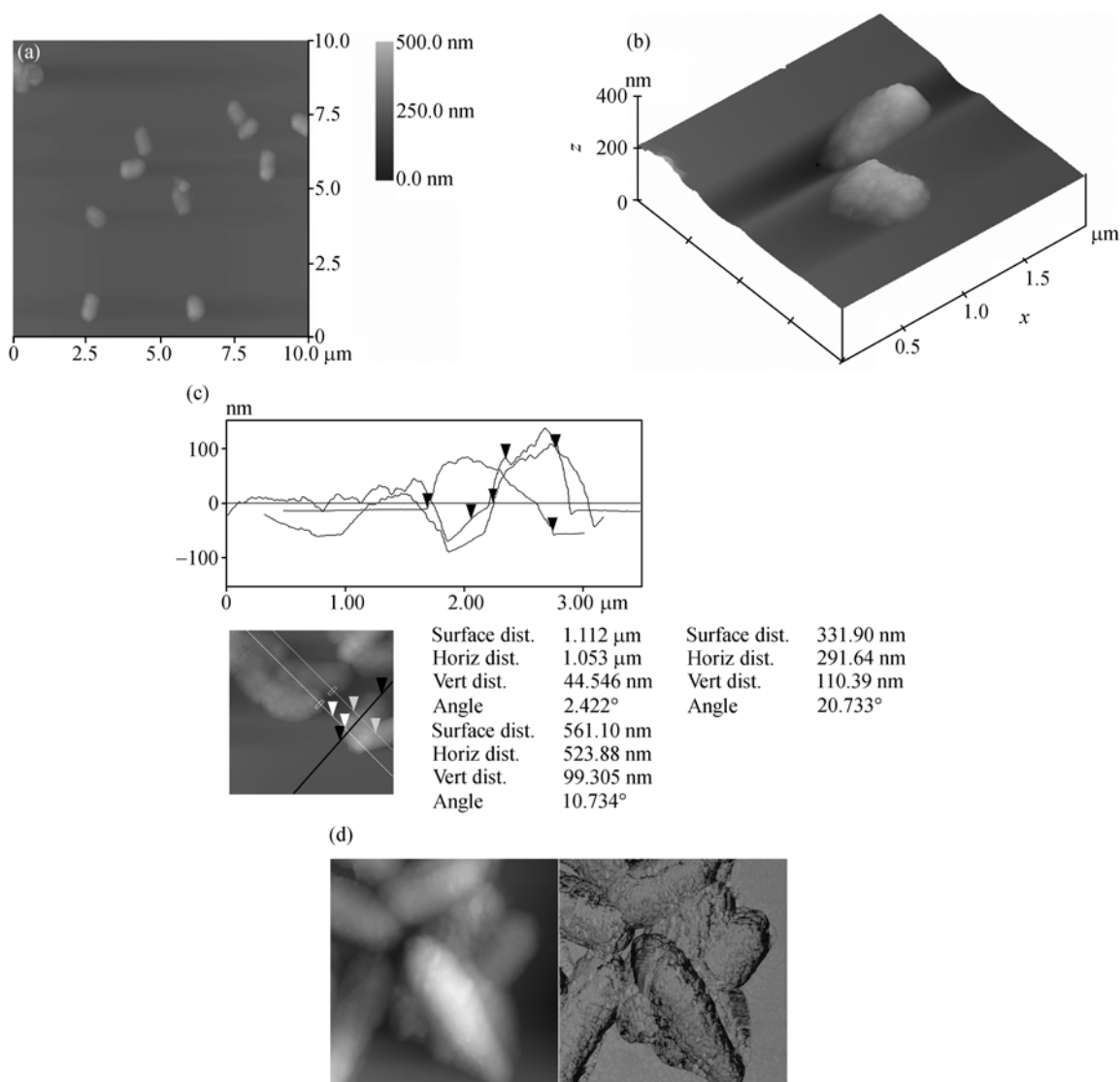


Figure 5 AFM characterization of metallized bacterial cells. (a) Height image of a large area showing several disperse metallized bacterial cells; (b) 3D height image of smaller area magnified from (a); (c) section analysis for one metallized *E. coli* cell, whose 3D size is 1053.0 \times 523.9 \times 110.4 nm; (d) phase image of metallized bacterial cells showing more morphological details, with the scan size being 1.64 \times 1.64 μm .

In conclusion, we had successfully fabricated hybrid nanomaterials with thin nickel coating using bacterial templates with electroless chemical plating, and characterized bare and metallized bacterial cells by using TEM and AFM. Compared with bare bacterial cells, some morphological changes have taken place for those after deposition with thin nickel coating, such as the ratio of height to width, and surface roughness. Based on the abundant morphological and microstructural information

supplied by advanced analytic techniques, it will be possible to study various and unique properties of this kind of hybrid nanomaterials, such as mechanical properties probed by nanoindentation^[20], and explore their potential application in nanoelectronics, nanomagnetism and nanomechanics in the future.

The authors would like to thank Xu Aiqun for TEM measurement and valuable discussion.

- 1 Ely O, Pan C, Amiens C, et al. Nanoscale bimetallic Co,Pt_{1-x} particles dispersed in poly(vinylpyrrolidone): synthesis from organometallic precursors and characterization. *J Phys Chem B*, 2000, 104(4): 695–702
- 2 Schmid G, Chi L F. Metal clusters and colloids. *Adv Mater*, 1998, 10: 515–526
- 3 Braun E, Eichen Y, Sivan U, et al. DNA-templated assembly and electrode attachment of a conducting silver wire. *Nature*, 1998, 391: 775–778
- 4 Keren K, Krueger M, Gilad R, et al. Sequence-specific molecular lithography on single DNA molecules. *Science*, 2002, 297: 72–75
- 5 Ford W, Harnack O, Yasuda A, et al. Platinated DNA as precursors to templated chains of metal nanoparticles. *Adv Mater*, 2001, 13: 1793–1797
- 6 Kirsch R, Mertig M, Pompe W, et al. Three-dimensional metallization of microtubules. *Thin Solid Films*, 1997, 305: 248–253
- 7 Markowitz M, Baral S, Brandow S, et al. Palladium ion assisted formation and metallization of lipid tubules. *Thin Solid Films*, 1993, 224: 242–247
- 8 Mertig M, Kirsch R, Pompe W, et al. Fabrication of highly oriented nanocluster arrays by biomolecular templating. *Eur Phys J D*, 1999, 9: 45–48
- 9 Wong K K W, Mann S. Biomimetic synthesis of cadmium sulfide-ferritin nanocomposites. *Adv Mater*, 1996, 8: 928–931
- 10 Xu L N, Zhou K C, Xu H F, et al. Copper thin coating deposition on natural pollen particles. *App Surf Sci*, 2001, 183: 58–61
- 11 Li X F, Li Y Q, Cai J, et al. Metallization of bacteria cells. *Sci China Ser E-Tech Sci*, 2003, 46(2): 161–167
- 12 Berry V, Saraf R F. Self-assembly of nanoparticles on live bacterium: an avenue to fabricate electronic devices. *Angew Chem Int Ed*, 2005, 44: 6668–6673
- 13 Berry V, Rangaswamy S, Saraf R F. Highly selective, electrically conductive monolayer of nanoparticles on live bacteria. *Nano Lett*, 2004, 4(5): 939–942
- 14 Amiel C, Mariey L, Denis C, et al. FTIR spectroscopy and taxonomic purpose: contribution of the classification of lactic acid bacteria. *J Travert*, 2001, 81: 249–255
- 15 Curk M C, Peladan F, Hubert J C. Fourier transform infrared (FTIR) spectroscopy for identifying lactobacillus species. *FEMS Microbiol Lett*, 1994, 123: 241–248
- 16 Beveridge T J. Ultrastructure, chemistry, and function of the bacterial wall. *Int Rev Cytol*, 1981, 72: 229–317
- 17 Beech I B. The potential use of atomic force microscopy for studying corrosion of metals in the presence of bacterial biofilms — An overview. *Int Biotet Biodeg*, 1996, 37: 141–149
- 18 Beech I B, Cheung C W S, Johnson D B, et al. Comparative studies of bacterial biofilms on steel surfaces using atomic force microscopy and environmental scanning electron microscopy. *Biofouling*, 1996, 10: 65–77
- 19 Grantham M C, Dove P M. Bacterial-mineral interactions: investigations using Fluid Tapping Mode atomic force microscopy. *Geochim Cosmochim Acta*, 1996, 60: 2473–2480
- 20 Wang J, He S Y, Xu L N, et al. Probing nanomechanical properties of nickel coated bacteria by nanoindentation. *Mater Lett*, 2006, 61(3): 917–920